Volume 1 | Number 1 | Jan 2013 | Pages 1–100

ChemComm

Chemical Communications
www.rsc.org/chemcomm

ROYAL SOCIETY
OF CHEMISTRY

This is an *Accepted Manuscript*, which has been through the Royal Society of Chemistry peer review process and has been accepted for publication.

Accepted Manuscripts are published online shortly after acceptance, before technical editing, formatting and proof reading. Using this free service, authors can make their results available to the community, in citable form, before we publish the edited article. We will replace this *Accepted Manuscript* with the edited and formatted *Advance Article* as soon as it is available.

You can find more information about *Accepted Manuscripts* in the **Information for Authors**.

Please note that technical editing may introduce minor changes to the text and/or graphics, which may alter content. The journal's standard **Terms & Conditions** and the **Ethical guidelines** still apply. In no event shall the Royal Society of Chemistry be held responsible for any errors or omissions in this *Accepted Manuscript* or any consequences arising from the use of any information it contains.

Journal Name

COMMUNICATION

Introduction of Mediator for Enhancing Photocatalytic Performance via Post-Synthetic Metal Exchange in Metal-Organic Frameworks (MOFs)

Dengrong Sun,[a] Wenjun Liu,[a] Mei Qiu,[b] Yongfan Zhang,[*,b] Zhaohui Li[*,a,b]

Ti-substituted NH₂-Uio-66(Zr/Ti) prepared by post-synthetic exchange (PSE) method showed enhanced photocatalytic performance for both CO₂ reduction and hydrogen evolution under visible light. Density functional theory (DFT) calculations and electron spin resonance (ESR) results reveal that the introduced Ti substituent acts as mediator to facilitate the electron transfer, which results in the enhanced performance.

The ever-increasing global demand for energy has stimulated a new wave of research activities on clean and renewable energy.[1] Heterogeneous photocatalysis is an ideal method to solve the energy problem since it can utilize the abundant solar energy.[2] Semiconductors are extensively studied photocatalysts, while metal-organic frameworks (MOFs), which have already shown potentials in a variety of applications, are emerging as a new type of promising photocatalysts.[3-7] However, only limited MOF-based photocatalytic systems have been developed and their efficiency is far from satisfactory.

Metal doping has already been demonstrated to be an effective method in enhancing the performance of semiconductor-based photocatalysts.[8] Introduction of the metal-to-metal charge transfer (MMCT) by metal substitution to construct bimetallic assemblies in semiconductor can lead to its enhanced photocatalytic performance, especially in the visible light region. Such bimetallic assemblies can harvest visible light and the doped metal cation can act as electron mediator to facilitate the charge transfer, which is beneficial for the photocatalysis. The introduction of metal as mediator via building similar hetero-bimetallic assemblies in zeolites has also been demonstrated and zeolite-anchored bimetallic assemblies have already been applied for photocatalytic CO₂ reduction, hydrogen evolution and alcohol oxidation.[9] Although bimetallic assemblies on semiconductors and zeolites have been shown to be promising for photocatalysis, the direct constructions of bimetallic assemblies with precise structure on these substrates are not straightforward. In contrast, MOFs, typically constructed from metal oxo-clusters interconnected by poly-dentate organic ligands, have definite composition and structure. The partial substitution of metal cations in MOFs can lead to the formation of oxo-bridged hetero-metallic assembly within the same MOFs.[10] Such bimetallic assemblies, similar to those constructed over semiconductors and zeolites but with more flexibility and tunability due to the availability of different MOF structures, are expected to show enhanced photocatalytic performance.

Inspired by the above assumption, herein we prepared Ti substituted NH₂-Uio-66(Zr) (denoted as NH₂-Uio-66(Zr/Ti)) via post-synthetic exchange (PSE) method and investigated their photocatalytic activities. It was found that NH₂-Uio-66(Zr/Ti) shows enhanced performance for both photocatalytic CO₂ reduction and hydrogen evolution. An enhanced mechanism over NH₂-Uio-66(Zr/Ti) was proposed based on the results of the density functional theory (DFT) calculations. This is the first demonstration that the construction of the bimetallic assembly via metal substitution in MOFs is an effective way to improve the photocatalytic performance of MOFs.

Ti-substituted NH₂-Uio-66(Zr) (denoted as NH₂-Uio-66(Zr/Ti)-T-t, where T represents the incubation temperature and t stands for the incubation time) were prepared via a PSE method by exposing NH₂-Uio-66(Zr) to DMF solution containing TiCl₄(THF)₂. It was found that during the incubation period, the original yellow color of the solution faded while in the meantime the color of the solid became deepened, implying the incorporation of Ti moiety in NH₂-Uio-66(Zr) (Fig. 1a inset). As shown in Table S1, for the incubation occurring at 100ºC for 4 days, the solid product contains 34.2% of Ti, while the amount of Zr in the solution corresponds to 29.3% of Zr in NH₂-Uio-66(Zr). This suggests that Zr in the original NH₂-Uio-66(Zr) has been substituted by Ti. The rate of the exchange was found to be influenced by the incubation temperature. For the exchange taking place at 120 °C, the solid obtained after a similar

time (4 days) contains 53.4 % of Ti, while about 46.5% of Zr in NH_2-Uio-66(Zr) had been exchanged into the solution. Therefore, to ensure a fast and efficient exchange process, 120°C was selected to prepare Ti-substituted NH_2-Uio-66(Zr) and the exchange process was monitored by ICP. As shown in Fig. 1a, the amount of Ti in the as-obtained solid increased sharply in the first 4days of incubation and fluctuated in a prolonged incubation time, reaching saturation with about 57% of Ti in 16 days. In the meantime, the concentration of Zr in the solution increased with incubation time and about 48.7% of Zr in NH_2-Uio-66(Zr) was replaced by Ti moiety after 16 days exchange. The slightly lower of the Zr content in the solution than the exchanged Ti moiety in NH_2-Uio-66(Zr/Ti) is probably caused by the adsorption of Zr moiety by the solid. The X-ray photoelectron spectrum (XPS) of NH_2-Uio-66(Zr/Ti)-120-16 in Ti 2p region shows two peaks at 458.7eV and 464.5eV, corresponding to Ti $2p_{3/2}$ and Ti $2p_{1/2}$ respectively, another confirmation of the successful incorporation of Ti moiety in NH_2-Uio-66(Zr) (Fig. 1b). The morphology of NH_2-Uio-66(Zr) was retained after the PSE process, suggesting that Ti was truly substituted into NH_2-UiO-66(Zr) framework (Fig. S1). The good agreement between the XRD patterns of NH_2-Uio-66(Zr/Ti)-120-16 and pristine NH_2-Uio-66(Zr) indicates that the framework of NH_2-Uio-66(Zr) is not collapsed and rules out the possibility of the formation of Ti-based impurities (Fig. 1c). However, as compared to original NH_2-Uio-66(Zr), the 2θ value at around 7.3° observed over NH_2-Uio-66(Zr/Ti)-120-16 shifts to higher value. Such phenomena are frequently observed over inorganic semiconductor solid solutions and suggest the substitution of larger Zr^{4+} in Zr-O oxo-clusters by smaller Ti^{4+}, which results in the shrinking of the crystal lattice.[11] The absence of amorphous Ti moiety was confirmed by the N_2 adsorption/desorption isotherms (Fig. S2). NH_2-Uio-66(Zr/Ti)-120-16 shows a BET specific surface area of 787 m^2g^{-1}, which is comparable with that observed over un-substituted NH_2-Uio-66(Zr) (778 m^2g^{-1}). Similar to un-substituted NH_2-Uio-66(Zr), the UV-visible diffuse-reflectance spectra (DRS) of NH_2-Uio-66(Zr/Ti)-120-16 also shows two main absorption peaks at around 265 and 365 nm (Fig. 1d). However, as compared with the un-substituted one, the peak at 265 nm, which is ascribed to the Zr-O clusters absorption in the NH_2-Uio-66(Zr), becomes broader. This broadening may be attributed to the absorption of Ti-O oxo-clusters generated by Ti substitution in NH_2-Uio-66(Zr/Ti) since similar peak broadening is also observed over the Ti-substituted Uio-66(Zr) without amine functionality (Fig. S3). In addition to the main peak at 365 nm, a shoulder peak extending to ca. 500 nm also emerges in NH_2-Uio-66(Zr/Ti)-120-16. Since the peak at 365 nm in NH_2-Uio-66(Zr) is ascribed to the ligand-based absorption influenced by the nearby metal center, the extending absorption in NH_2-Uio-66(Zr/Ti)-120-16 can be assigned to the interaction between the ligand and substituted Ti centers. All these characterizations indicate that part of Zr^{4+} have been successfully substituted by Ti^{4+} in NH_2-Uio-66(Zr/Ti)-120-16.

Actually, the successful substitution of Zr by Ti was also supported by the X-ray absorption fine structure (XAFS) analyses (Fig. S4 and Table S2). The local environment of Zr in NH_2-Uio-66(Zr) is eight-fold coordinated with two short (2.06Å) and six long (2.27 Å) Zr-O bond, in agreement with the previous report (Fig. S4a, Table S2).[12] Similar coordination environment was observed on the Ti in NH_2-Uio-66(Zr/Ti)-120-16, indicating that Ti is truly substituted into the NH_2-Uio-66(Zr) framework (Fig. S4b, Table S2). No observation of peaks corresponding to other Ti species ruled out the presence of adsorbed Ti or Ti-based impurities.

To study the influence of Ti substitution on the photocatalysis of NH_2-Uio-66(Zr), the photocatalytic performance for CO_2 reduction over the as-prepared NH_2-Uio-66(Zr/Ti)-120-16 was investigated. Triethanolamine (TEOA) was chosen as sacrificial

agent, which acts as both an electron donor and hydrogen donor and provides basic environment to facilitate the photocatalytic CO_2 reduction. Similar with NH_2-Uio-66(Zr), NH_2-Uio-66(Zr/Ti)-120-16 also showed photocatalytic activity for CO_2 reduction to give $HCOO^-$ under visible-light irradiation. No gas products such as CO, methane, ethane or hydrogen were detected. As shown in Fig. 2a, the produced $HCOO^-$ increased almost linearly with time and about 5.8 $mmol^.mol^{-1}$ of $HCOO^-$ was produced over NH_2-Uio-66(Zr/Ti)-120-16 after 10h irradiation, 1.7 times as that observed over NH_2-Uio-66(Zr) (3.4 $mmol^.mol^{-1}$) under otherwise similar condition. No formate was formed in absence of either the photocatalyst or CO_2. The reaction carried out using $^{13}CO_2$ over the MOFs confirmed the source of the formate to be CO_2 (Fig. S5). No decomposition of the formate was observed due to the basic medium. XRD and N_2 adsorption/desorption isotherms analyses of NH_2-Uio-66(Zr/Ti)-120-16 after reaction showed that NH_2-Uio-66(Zr/Ti)-120-16 is stable during the photoreaction of CO_2 (Fig. S6). Although NH_2-Uio-66(Zr/Ti)-120-16 exhibits a higher CO_2 adsorption capacity of 83 cm^3g^{-1} as compared with that observed over NH_2-Uio-66(Zr) (68 cm^3g^{-1}), the improvement in its photocatalytic activity for CO_2 reduction can not be simply explained in terms of its enhanced CO_2 adsorption capacity (Fig. S7). Controlled experiment reveals that NH_2-Uio-66(Zr/Ti)-100-4, with a comparable CO_2 adsorption capability (80 cm^3g^{-1}), produce only 4.2 $mmol^.mol^{-1}$ of $HCOO^-$ in a similar reaction time. This value is also higher than that over pristine NH_2-Uio-66(Zr), but with a less improvement extent as compared to that NH_2-Uio-66(Zr/Ti)-120-16. This indicates that in addition to the CO_2 adsorption capability, factor related to the incorporated Ti moiety may account for the improved photocatalytic performance of NH_2-Uio-66(Zr/Ti).
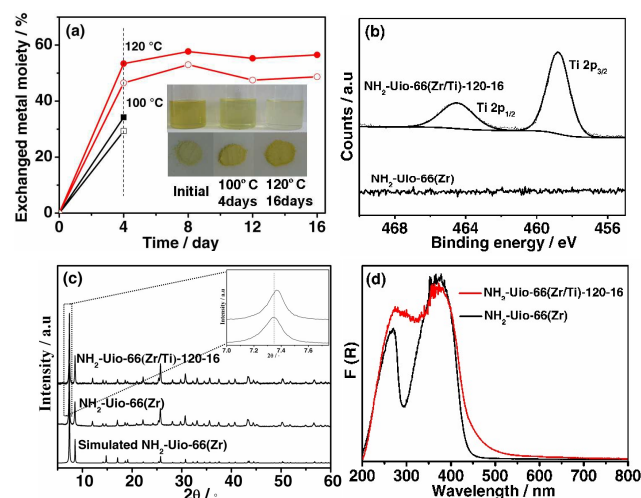

Fig. 1 (a) Change of the amount of Ti moiety in solids with incubation period at 120°C (●) and 100°C (■); the amount of Zr moiety in the solutions with incubation period at 120°C (○) and 100°C (□) (inset) Photographs showing the solutions and solids after different incubation period; (b) XPS spectra of NH_2-Uio-66(Zr/Ti)-120-16 and NH_2-Uio-66(Zr) in Ti 2p region; (c) XRD patterns of simulated NH_2-Uio-66(Zr) and prepared NH_2-Uio-66(Zr/Ti)-120-16 and NH_2-Uio-66(Zr); (d) UV/Vis spectra of NH_2-Uio-66(Zr/Ti)-120-16 and NH_2-Uio-66(Zr).

NH_2-Uio-66(Zr/Ti)-120-16 also showed enhanced photocatalytic activity for hydrogen evolution with TEOA as electron donor under visible light irradiation. As shown in Fig. 2b, only about 2.4 $mmol^.mol^{-1}$ H_2 was detected over Pt/NH_2-Uio-66(Zr) after 9h visible light irradiation. However, 3.5 $mmol^.mol^{-1}$ of H_2 was produced over Pt/NH_2-Uio-66(Zr/Ti)-120-16 under similar condition, 1.5 times as that evolved over Pt/NH_2-Uio-66(Zr).
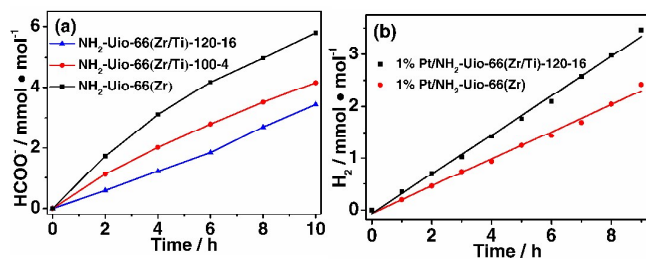
Fig. 2 (a) Amount of HCOO$^-$ produced as a function of irradiation time over different samples (Photocatalyst : 50 mg, MeCN/TEOA (5/1), solution volume: 60 mL); (b) Amount of hydrogen evolved during the photocatalytic reactions over different samples (Photocatalyst : 50 mg, solvent: H$_2$O, H$_2$O/TEOA (5/1), solution volume: 60 mL).
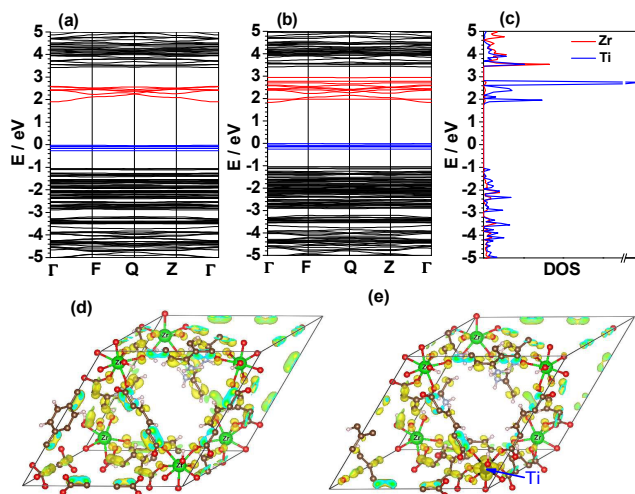

Fig. 3 (a) Band structure of NH$_2$-Uio-66(Zr); (b) Band structure of Ti-doped NH$_2$-Uio-66(Zr); (c) Partial density of states (DOSs) of Zr and Ti atoms in the Ti-doped NH$_2$-Uio-66(Zr), and the partial charge density map (drawn at isosurface level 0.01e/Å^3) of conduction band located in the region from 1.9 to 2.6 eV above the Fermi level for the (d) undoped and (e) Ti-doped NH$_2$-Uio-66(Zr)s. In Figures a~c, the Fermi level is set to zero.

These results indicated that the incorporated Ti moiety is beneficial for the photocatalysis over NH$_2$-Uio-66(Zr/Ti). To elucidate how the enhancement occurs over NH$_2$-Uio-66(Zr/Ti), the electronic structures of un-doped and Ti-doped NH$_2$-Uio-66(Zr) were studied by DFT calculations. The density of states (Fig. S8) and the band structure (Fig. 3a) of pure NH$_2$-Uio-66(Zr) reveal that the valence band near the Fermi level is mainly derived from the 2p states (lone pairs) of nitrogen atoms, while the bottom of the conduction band is dominated by the π* states of the ligand 2-aminoterephthalic acid (ATA), without the contributions of Zr atoms (Fig. 3d). When Ti dopant is introduced, several energy bands appear in the conduction band of Ti-doped NH$_2$-Uio-66(Zr) (Fig. 3b). Partial density of states (DOSs) of Zr and Ti atoms shows that although the arrangements of the electronic states of Ti and Zr atoms are similar, Ti atoms make significant contributions to the bottom of the conduction band of Ti-doped NH$_2$-Uio-66(Zr) (Fig. 3c and 3e). Therefore, the theoretical results indicate a favorable electron transfer from excited ATA to Ti moiety to form (Ti^{3+}/Zr^{4+})$_6$O$_4$(OH)$_4$ in Ti-doped NH$_2$-Uio-66(Zr). However, due to the overlap of the electronic states of Zr and Ti atoms (mainly located in the region from 3.4 to 4.6 eV) in Ti-doped NH$_2$-Uio-66(Zr), Ti^{3+} can further transfer electrons to Zr^{4+} to form the photocatalytic active Zr^{3+}. Thus, it is inferred that the substituted Ti moieties may act as electron mediator in promoting the electron transfer from ATA to Zr center.

The Ti-mediated electron transfer was further confirmed by in-situ low temperature ESR analyses. To ensure a successful observation of Ti^{3+} to Zr^{4+} charge transfer, the ESR experiment was carried out at 250K to slow down the rate of electron transfer. ESR study showed that Zr^{3+} (g value at 2.002) can be formed over irradiated NH$_2$-Uio-66(Zr), which is responsible for the CO$_2$ reduction (Fig. S9a).[7c] The intensity of the as-formed Zr^{3+} signal remained unchanged after the irradiation was switched off, indicating that the as-formed Zr^{3+} was stable under this condition (Fig. S9a). For NH$_2$-Uio-66(Zr/Ti), in addition to the Zr^{3+} signal, another ESR signal at g value of 1.944 emerged under similar condition, which can be assigned to the Ti^{3+} moiety (Fig. S9b). The formation of Ti^{3+} moiety is in accordance with the color change from yellow to green for NH$_2$-Uio-66(Zr/Ti) suspension when irradiated (Fig. S10).[7a,13] Unlike that in NH$_2$-Uio-66(Zr), the intensity of Zr^{3+} signal in NH$_2$-Uio-66(Zr/Ti) gradually increased after light was switched off, while the intensity of Ti^{3+} signal decreased (Fig. S9b). This observation clearly suggests that Ti^{3+} donates an electron to Zr^{4+} to promote the formation of Zr^{3+}, ie, Ti acts as a mediator during the photocatalysis over NH$_2$-Uio-66(Zr/Ti).

Therefore, the enhancement of the photocatalytic performance over Ti-substituted NH$_2$-Uio-66(Zr/Ti) can be well explained based on the experimental observations and theoretical calculations. As previously reported on the photocatalytic CO$_2$ reduction over NH$_2$-Uio-66(Zr), the ligand ATA is excited upon visible light irradiation and the excited ATA can transfer electrons to the Zr-O oxo-metal clusters Zr$_6$O$_4$(OH)$_4$, the node in NH$_2$-Uio-66(Zr).[7c,14] In this way, Zr^{4+} is reduced to Zr^{3+}, which is active for the photocatalytic CO$_2$ reduction to form HCOO$^-$. When part of Zr^{4+} centers in Zr$_6$O$_4$(OH)$_4$ are substituted by Ti^{4+} to form (Ti/Zr)$_6$O$_4$(OH)$_4$, the excited ATA can transfer electrons to either Zr^{4+} or Ti^{4+} centers. According to the theoretical studies, the probability for the electrons transferred to Ti^{4+} is higher than that to Zr^{4+} centers and thus the formation of excited (Ti^{3+}/Zr^{4+})$_6$O$_4$(OH)$_4$ is expected. Such oxo-bridged Ti^{3+}-O-Zr^{4+} in NH$_2$-Uio-66(Zr/Ti) is similar to those previously reported zeolite-anchored Cu$^+$-O-Zr^{4+} and Ti^{3+}-O-Ce^{4+} or Fe^{2+}-O-Ti^{4+} in Fe-substituted SrTiO$_3$.[8e,9a,9b] The Ti^{3+} in excited (Ti^{3+}/Zr^{4+})$_6$O$_4$(OH)$_4$ can act as an electron donor that donates electrons to Zr^{4+} to form Ti^{4+}-O-Zr^{3+}. Such an electron transfer mechanism is similar to those observed previously over zeolite-anchored bimetallic assemblies or Fe-doped SrTiO$_3$ and can also be utilized for an enhanced photocatalysis in visible light region.[8e,9] In this regard, the substituted Ti center in NH$_2$-Uio-66(Zr/Ti) helps to improve the interfacial charge transfer from excited ATA to Zr-O oxo-clusters which is beneficial for the visible light photocatalysis (Scheme 1).
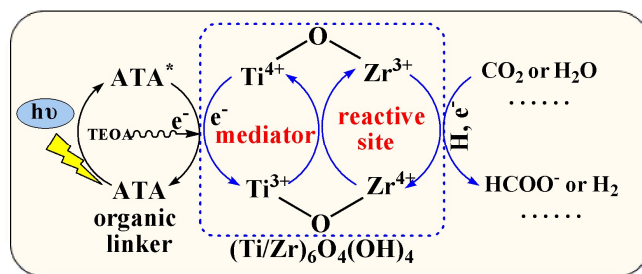
Scheme 1. Proposed enhanced mechanism for the photocatalytic reactions over NH$_2$-Uio-66(Zr/Ti).

In summary, Ti-substituted NH$_2$-Uio-66(Zr/Ti) prepared by PSE method showed enhanced photocatalytic performance via a Ti-mediated electron transfer mechanism. This study proposed an effective method to enhance the performance of MOF-based photocatalysts. The only limitation in the current system is the use of TEOA, which is not so green and

economical. To find some stable MOFs which can sustain the photocatalytic reaction in water is indispensable but promising if we consider the variety of MOFs structures. The facile realization of metal substitution in MOFs and their structural diversity would allow us to develop a variety of MOF-based photocatalysts with desired performance in a more controllable way. The strategy to improve the photocatalytic activity via PSE in the current work is believed to be a general method to develop highly efficient photocatalyst. This work would certainly activate intensive research on MOFs-based photocatalysis and also open a new prospect for the development of molecular-based photocatalysis.

Notes and references

[a] D. Sun, W. Liu, Prof. Dr. Z. Li

Research Institute of Photocatalysis

State Key Laboratory of Photocatalysis on Energy and Environment

Fuzhou University, Fuzhou, 350002 (P.R. China)

E-mail: zhaohuili1969@yahoo.com (Z. Li).

[b] M. Qiu, Prof. Dr. Y. Zhang, Prof. Dr. Z. Li

College of Chemistry

Fuzhou University, Fuzhou, 350002 (P.R. China)

E-mail: zhangyf@fzu.edu.cn (Y. Zhang).

Electronic Supplementary Information (ESI) available: The details of synthesis, complete characterization and computational details of the products can be found in the Supporting Information. See DOI: 10.1039/c000000x/

1   (a) A. Kubacka, M. Fernández-García and G. Colón, *Chem. Rev.,* 2012, **112**, 1555; (b) H. Chen, C. E. Nanayakkara and V. H. Grassian, *Chem. Rev.,* 2012, **112**, 5919; (c) A. J. Esswein and D. G. Nocera, *Chem. Rev.,* 2007, **107**, 4022.

2   (a) A. M. Appel, J. E. Bercaw, A. B. Bocarsly, H. Dobbek, D. L. DuBois, M. Dupuis, J. G. Ferry, E. Fujita, R. Hille, P. J. A. Kenis, C. A. Kerfeld, R. H. Morris, C. H. F. Peden, A. R. Portis, S. W. Ragsdale, T. B. Rauchfuss, J. N. H. Reek, L. C. Seefeldt, R. K. Thauer and G. L. Waldrop, *Chem. Rev.,* 2013, **113**, 6621; (b) W. Wang, S. Wang, X. Ma and J. Gong, *Chem. Soc. Rev.,* 2011, **40**, 3703; (c) X. Chen, S. Shen, L. Guo and S. S. Mao, *Chem. Rev.,* 2010, **110**, 6503; (d) X. Lang, X. Chen and J. Zhao, *Chem. Soc. Rev.,* 2014, **43**, 473.

3   (a) G. Férey, C. Serre, T. Devic, G. Maurin, H. Jobic, P. L. Llewellyn, G. D. Weireld, A. Vimont, M. Daturi and J. S. Chang, *Chem. Soc. Rev.,* 2011, **40**, 550; (b) T. R. Cook, Y. R. Zheng and P. J. Stang, *Chem. Rev.,* 2013, **113**, 734.

4   (a) J. R. Li, J. Sculley and H. C. Zhou, *Chem. Rev.,* 2012, **112**, 869; (b) L. J. Murray, M. Dinca and J. R. Long, *Chem. Soc. Rev.,* 2009, **38**, 1294; (c) J. L. C. Rowsel and, O. M. Yaghi, *Angew. Chem. Int. Ed.,* 2005, **44**, 4670; (d) R. Matsuda, R. Kitaura, S. Kitagawa, Y. Kubota, R. V. Belosludov, T. C. Kobayashi, H. Sakamoto, T. Chiba, M. Takata, Y. Kawazoe and Y. Mita, *Nature,* 2005, **436**, 238; (e) B. Chen, S. Xiang and G. Qian, *Acc. Chem. Res.,* 2010, **43**, 1115.

5   (a) A. Corma, H. García and F. X. Llabres i Xamena, *Chem. Rev.,* 2010, **110**, 4606; (b) J. Lee, O. K. Farha, J. Roberts, K. A. Scheidt, S. T. Nguyen and J. T. Hupp, *Chem. Soc. Rev.,* 2009, **38**, 1450; (c) W. Xuan, C. Zhu, Y. Liu and Y. Cui, *Chem. Soc. Rev.,* 2012, **41**, 1677; (d) W.-Y. Gao, M. Chrzanowski and S. Ma, *Chem. Soc. Rev.*, 2014, **43**, 5841.

6   (a) P. Horcajada, R. Gref, T. Baati, P. K. Allan, G. Maurin, P. Couvreur, G. Férey, R. E. Morris and C. Serre, *Chem. Rev.,* 2012, **112**, 1232; (b) K. M. L. Taylor-Pashow, J. D. Rocca, Z. Xie, S. Tran and W. Lin, *J. Am. Chem. Soc.,* 2009, **131**, 14261.

7   (a) Y. Fu, D. Sun, Y. Chen, R. Huang, Z. Ding, X. Fu and Z. Li, *Angew. Chem. Int. Ed.,* 2012, **51**, 3364; (b) D. Sun, W. Liu, Y. Fu, Z. Fang, F. Sun, X. Fu, Y. Zhang and Z. Li, *Chem.-Eur. J.,* 2014, **20**, 4780; (c) D. Sun, Y. Fu, W. Liu, L. Ye, D. Wang, L. Yang, X. Fu and Z. Li, *Chem.-Eur. J.,* 2013, **19**, 14279; (d) S. Li and Q. Xu, *Energy Environ. Sci.,* 2013, **6**, 1656; (e) M. C. Das, H. Xu, Z. Wang, G. Srinivas, W. Zhou, Y. F. Yue, V. N. Nesterov, G. Qian and B. Chen, *Chem. Commun.,* 2011, **47**, 11715; (f) T. Zhang and W. Lin, *Chem. Soc. Rev.,* 2014, **43**, 5982.

8   (a) I. Tsuji, H. Kato, H. Kobayashi and A. Kudo, *J. Am. Chem. Soc.,* 2004, **126**, 13406; (b) W. Zhang, Z. Zhong, Y. Wang and R. Xu, *J. Phys. Chem. C,* 2008, **112**, 17635; (c) Y. Huang, Z. Zheng, Z. Ai, L. Zhang, X. Fan and Z. Zou, *J. Phys. Chem. B,* 2006, **110**, 19323; (d) T.-H. Xie, X. Sun and J. Lin, *J. Phys. Chem. C,* 2008, **112**, 9753.

9   (a) W. Lin and H. Frei, *J. Am. Chem. Soc.,* 2005, **127**, 1610; (b) R. Nakamura, A. Okamoto, H. Osawa, H. Irie and K. Hashimoto, *J. Am. Chem. Soc.,* 2007, **129**, 9596; (c) H. Han and H. Frei, *J. Phys. Chem. C,* 2008, **112**, 8391.

10   (a) S. Das, H. Kim and K. Kim, *J. Am. Chem. Soc.,* 2009, **131**, 3814; (b) C. K. Brozek and M. Dinca, *J. Am. Chem. Soc.,* 2013, **135**, 12886; (c) M. Kim, J. F. Cahill, H. Fei, K. A. Prather and S. M. Cohen, *J. Am. Chem. Soc.,* 2012, **134**, 18082; (d) C. H. Lau, R. Babarao and M. R. Hill, *Chem. Commun.,* 2013, **49**, 3634.

11   Y.-F. Li, D. Xu, J. I. Oh, W. Shen, X. Li and Y. Yu, *ACS Catal.* 2012, **2**, 391.

12   L. Valenzano, B. Civalleri, S. Chavan, S. Bordiga, M. H. Nilsen, S. Jakobsen, K. P. Lillerud and C. Lamberti, *Chem. Mater.,* 2011, **23**, 1700.

13   M. Dan-Hardi, C. Serre, T. Frot, L. Rozes, G. Maurin, C. Sanchez and G. Férey, *J. Am. Chem. Soc.,* 2009, **131**, 10857.

14   J. H. Cavka, S. Jakobsen, U. Olsbye, N. Guillou, C. Lamberti, S. Bordiga and K. P. Lillerud, *J. Am. Chem. Soc.,* 2008, **130**, 13850.

ChemComm Accepted Manuscript